

Postsystolic Shortening in Ischemic Myocardium Active Contraction or Passive Recoil?

Helge Skulstad, MD; Thor Edvardsen, MD; Stig Urheim, MD; Stein Inge Rabben, PhD;
Marie Stugaard, PhD, MD; Erik Lyseggen, MD; Halfdan Ihlen, PhD, MD; Otto A. Smiseth, PhD, MD

Background—Postsystolic shortening in ischemic myocardium has been proposed as a marker of tissue viability. Our objectives were to determine if postsystolic shortening represents active fiber shortening or passive recoil and if postsystolic shortening may be quantified by strain Doppler echocardiography (SDE).

Methods and Results—In 15 anesthetized dogs, we measured left ventricular (LV) pressure, myocardial long-axis strains by SDE, and segment lengths by sonomicrometry before and during LAD stenosis and occlusion. Active contraction was defined as elevated LVP and stress during postsystolic shortening when compared with the fully relaxed ventricle at similar segment lengths. LAD stenosis decreased systolic shortening from $10.4 \pm 1.2\%$ to $5.9 \pm 0.9\%$ ($P < 0.05$), whereas postsystolic shortening increased from $1.1 \pm 0.3\%$ to $4.2 \pm 0.7\%$ ($P < 0.05$). In hypokinetic and akinetic segments, LV pressure–segment length and LV stress–segment length loop analysis indicated that postsystolic shortening was active. LAD occlusion resulted in dyskinesis, and postsystolic shortening increased additionally to $8.2 \pm 1.0\%$ ($P < 0.05$). After 3 to 5 minutes with LAD occlusion, the dyskinetic segment generated no active stress, and the postsystolic shortening was attributable to passive recoil. Elevation of afterload caused hypokinetic segments to become dyskinetic, and postsystolic shortening remained partly active. Postsystolic shortening by SDE correlated well with sonomicrometry ($r = 0.83$, $P < 0.01$).

Conclusions—Postsystolic shortening is a relatively nonspecific feature of ischemic myocardium and may occur in dyskinetic segments by an entirely passive mechanism. However, in segments with systolic hypokinesis or akinesis, postsystolic shortening is a marker of actively contracting myocardium. SDE was able to quantify postsystolic shortening and might represent a clinical method for identifying actively contracting and hence viable myocardium. (*Circulation*. 2002;106:718-724.)

Key Words: echocardiography ■ ischemia ■ ventricles ■ myocardial contraction

The assessment of myocardial viability in patients with acute coronary syndrome is a major diagnostic challenge. It has been proposed that postsystolic (postejection) shortening may serve as a marker of actively contracting and therefore viable myocardium.^{1,2} In keeping with this, Gibson et al³ observed in a clinical angiographic study that hypokinesis combined with delayed inward wall motion was associated with recovery of left ventricular (LV) function after thrombolysis. In a more recent clinical study, Hosokawa et al⁴ claimed that postsystolic shortening as measured by angiography represents actively contracting myocardium. Implementation of this concept in clinical routine, however, requires a method that can quantify postsystolic shortening noninvasively. Measurement of myocardial strain by Doppler echocardiography (SDE) may represent such a method.⁵⁻⁹

The objectives of the present experimental study were to determine if SDE can quantify postsystolic shortening and to examine the validity of the concept that postsystolic shorten-

ing is a marker of actively contracting myocardium, as opposed to being a nonspecific finding in ischemic myocardium. Classification of myocardial shortening as passive or active was done by assessment of regional myocardial work, calculated as the area of the myocardial pressure–segment length loop. In addition, we compared the elastic properties of the myocardium during postsystolic shortening with elastic properties in late diastole, when the myocardium is presumably fully relaxed. The rationale for the latter approach is that an active component will result in a stiffer myocardium than predicted by the pressure-dimension relationship of the fully relaxed myocardium. To account for the confounding effect of changes in LV geometry on the pressure-dimension analysis, we also calculated regional stress and constructed stress–segment length loops.

The influence of loading conditions on contractile patterns was studied by changing aortic pressure. The experiments were done in acutely anesthetized dogs.

Received March 29, 2002; revision received May 7, 2002; accepted May 10, 2002.

From the Institute for Surgical Research and Department of Cardiology, Rikshospitalet University Hospital, Oslo, Norway.

Correspondence to Otto A. Smiseth, Department of Cardiology, Rikshospitalet University Hospital, N-0027 Oslo, Norway. E-mail o.a.smiseth@klinmed.uio.no

© 2002 American Heart Association, Inc.

Circulation is available at <http://www.circulationaha.org>

DOI: 10.1161/01.CIR.0000024102.55150.B6

Methods

Fifteen mongrel dogs of either sex and with body weight 20.7 ± 1.2 kg were anesthetized, ventilated, and surgically prepared as previously described.⁸ Pneumatic constrictors were positioned around the proximal part of the LAD and the ascending aorta. The dogs were placed in the left supine position during recordings. The National Animal Experimentation Board approved the study, and the laboratory animals were supplied by Avdeling for komparativ medisin, Rikshospitalet, the Netherlands.

Hemodynamic Measurements

Left atrial and LV pressures were measured by micromanometers and LAD flow by ultrasound transit time, as previously described,¹⁰ and data were digitized at 200 Hz.

Sonomicrometry

In the anterior LV wall (LAD region), one pair of ultrasonic crystals was implanted in the inner third of the myocardium, aligned parallel with the LV long axis. Another pair was implanted in the same region with one crystal in the epicardium and the other in the subendocardium to measure wall thickness. A pair of longitudinal crystals was positioned in the inner third of the posterior LV wall (circumflex artery region). The crystals were connected to a sonomicrometer (Sonometrics). To define local radius of curvature in the LAD region, we placed 4 additional crystals in the subepicardium with the epicardial wall thickness crystal in the center. One pair was aligned parallel to and one pair at a 90-degree angle to the subendocardial pair, and each crystal had a distance of 6 to 10 mm to the center crystal.

Echocardiography

We used a System FiVe digital ultrasound machine (GE Vingmed Ultrasound) with a combined tissue imaging (3.5 MHz) and Doppler (2.75 MHz) transducer. The mean frame rate was 85 per second. To minimize noise, the pulse repetition frequency was set to 0.5 to 1 kHz. Recordings were done from apical and short-axis views, and we oriented the image planes through the regions in which crystals were positioned.

Calculations

Longitudinal peak systolic shortening by sonomicrometry was calculated in percentage of end-diastolic dimension. Postsystolic shortening was calculated as segment shortening after LV dP/dt_{min} , in percentage of end-diastolic dimension.

Longitudinal shortening by SDE, evaluated as segmental strain, was calculated offline. Strain rate (SR) color-coded images were generated from tissue Doppler images (Figure 1) by calculating the velocity differences at positions 6 mm apart. From the strain rate data, segmental strain [$e = (L - L_0/L_0)$] was estimated as $e = \exp(\int SR dt) - 1$.^{7,8} For the purpose of this study, strain measurements were done only in the myocardial segment in which we had ultrasonic crystals.

To facilitate comparison between the methods, we report SDE and sonomicrometry data with similar terminology, ie, as systolic and postsystolic shortening. The areas of the LV pressure–segment length loops were calculated and were used as an index of regional segmental work.

Wall stresses were calculated by combining measurements of LV pressure, wall thickness, and radii of curvature with models for longitudinal wall stress σ_ϕ and average wall stress σ .^{11–13} The longitudinal and circumferential radii of curvature were calculated by fitting a circle to the 3 crystal positions in each direction. The positions of the crystals were calculated from all crystal-to-crystal distances. All values represent the mean of 3 consecutive heart cycles.

Experimental Protocol

After a 30-minute stabilization period, baseline recordings were performed. To avoid interference between sonomicrometry and

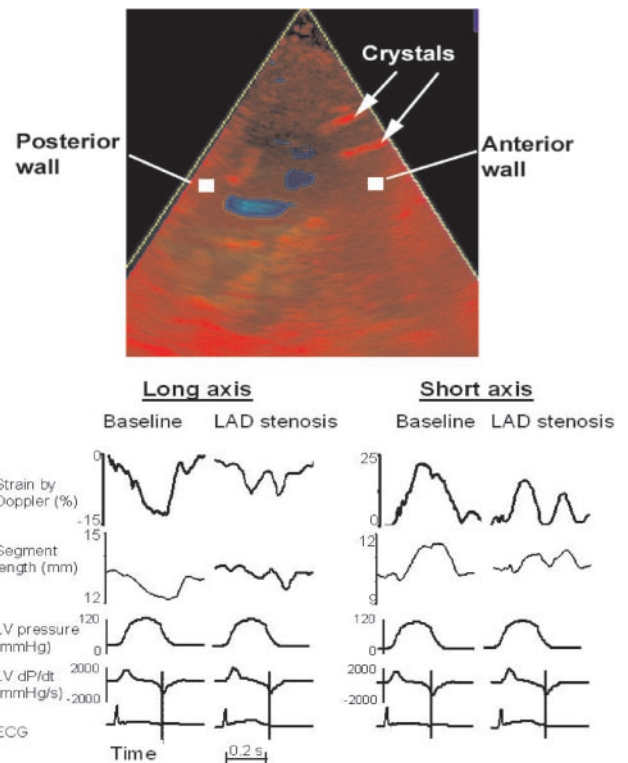


Figure 1. Representative tissue Doppler image showing the position of one pair of ultrasonic crystals (top) with accompanying recordings of myocardial function by SDE and sonomicrometry (bottom). SDE measurements were recorded from the myocardial segment between the crystals. Note the biphasic contractile pattern during LAD stenosis, with substantial post-systolic shortening and postsystolic thickening in the LV long and short axis, respectively. The time of peak negative dP/dt as a marker of global end-systole is indicated by the vertical lines.

Doppler, we first recorded pressures, ECG, and echocardiographic data during 10 seconds and then pressures, flow, ECG, and segment lengths during the subsequent 10 seconds. Data were recorded with the respirator off.

Myocardial Ischemia

In 10 dogs, LAD flow was reduced progressively until sonomicrometry showed marked hypokinesia. LAD flow was reduced by $47 \pm 6\%$. The hemodynamic variables were allowed to stabilize for 1 to 2 minutes before recordings were taken. Then the constrictor was deflated. After a recovery period, another set of baseline recordings were performed. In 7 dogs, LAD stenosis was reestablished, and hypokinesia was confirmed. During the LAD stenosis, we elevated LV afterload by instantly constricting the ascending aorta. After 10 seconds, the constrictor was deflated. After 30 minutes of reperfusion, which resulted in complete functional recovery, the LAD was occluded for 30 minutes. In a separate series of 5 dogs, the LAD stenosis was maintained for 30 minutes, and measurements were performed every 5 minutes.

Statistics

Values are expressed as mean \pm SEM. For multiple comparisons, nonparametric 2-way ANOVA was performed. Paired data were analyzed with Wilcoxon matched-pair test. Shortening values obtained by the 2 methods were compared by regression analysis with a least-squares method, and the method of Bland-Altman.¹⁴ $P < 0.05$ was considered significant.

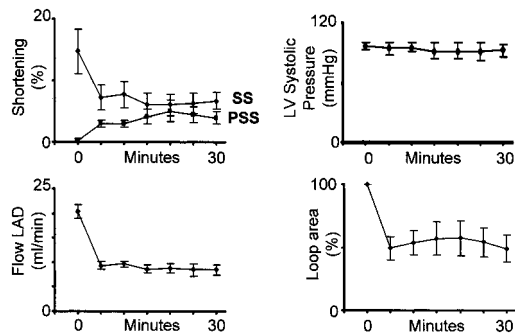


Figure 2. Regional myocardial function by sonomicrometry and LAD flow during 30 minutes with LAD stenosis. The postsystolic shortening persisted and the LV pressure–segment length loop area was essentially unchanged during this time period. PSS indicates postsystolic shortening; SS, systolic shortening.

Results

LAD Stenosis

As demonstrated by Figure 1, LAD stenosis resulted in a decrease in longitudinal systolic shortening and induced substantial postsystolic shortening. Similarly, in the short-axis view, there was reduced systolic myocardial thickening and substantial postsystolic thickening. This pattern was observed with SDE as well as with sonomicrometry and persisted for the entire 30-minute period with ischemia (Figure 2). In the rest of this report, we focus on long-axis measurements. Mean data are presented in Table 1.

When aortic constriction was superimposed on LAD stenosis, the pattern changed within 2 to 3 beats to systolic lengthening, and there was an additional increase in postsystolic shortening (Figure 3 and Table 2).

LAD Occlusion

LAD occlusion caused systolic lengthening, and the associated postsystolic shortening was larger than during LAD stenosis (Figure 3, Table 1). As demonstrated in Figure 3, the contractile pattern during combined LAD stenosis and aortic constriction resembles that during LAD occlusion.

Pressure–Segment Length Loops and Regional Wall Stress

Figure 4 shows that the induction of LAD stenosis caused a marked decrease in the area of the LV pressure–segment length loop. However, the loop continued to rotate counterclockwise, indicating that the segment still performed active work. Note also that the LV pressure–segment length relationship during isovolumic relaxation (IVR) is shifted upwards relative to the late diastolic parts of the loop. The upward shift was 19.7 ± 2.5 mm Hg at mid-IVR. During aortic constriction, when the segment was dyskinetic, the upward shift of the IVR segment persisted.

To investigate if the upward shift was present in segments with akinesia (pronounced hypokinesia), we selected 6 segments with systolic shortening $< \pm 3\%$. In these segments, there was an upward shift of 14.7 ± 1.5 mm Hg, and the upward shift was present to similar extent regardless of whether there was slight systolic shortening ($n=3$) or slight systolic lengthening ($n=3$).

TABLE 1. Hemodynamic Variables During Baseline, LAD Stenosis, and LAD Occlusion (n=10)

	Baseline	LAD Stenosis	LAD Occlusion
Heart rate, min^{-1}	107 ± 9	108 ± 9	109 ± 9
LV peak systolic pressure, mm Hg	101 ± 8	100 ± 7	105 ± 9
LV end-diastolic pressure, mm Hg	9 ± 2	9 ± 2	$11 \pm 2^{\dagger}$
LV dP/dt_{max} , mm Hg/s	1683 ± 125	$1455 \pm 91^*$	$1593 \pm 146^*$
LAD flow, mL/min \ddagger	13 ± 2	$7 \pm 1^*$	$0 \pm 0^{\dagger}$
End-diastolic segment length, mm			
LAD region	10.5 ± 1.2	10.5 ± 1.2	$10.8 \pm 1.2^{\dagger}$
Cx region	8.9 ± 1.0	8.9 ± 1.0	9.0 ± 1.0
Systolic shortening, LAD region, %			
Sonomicrometry	10.4 ± 1.2	$5.9 \pm 0.9^*$	$-6.0 \pm 0.7^{\dagger}$
Doppler	12.2 ± 0.9	$6.1 \pm 1.0^*$	$-7.7 \pm 1.0^{\dagger}$
Systolic shortening, Cx region, %			
Sonomicrometry \ddagger	14.3 ± 2.2	15.2 ± 2.7	13.7 ± 2.5
Doppler \ddagger	15.9 ± 1.8	13.4 ± 0.8	13.5 ± 1.0
Postsystolic shortening, LAD region, %			
Sonomicrometry	1.1 ± 0.3	$4.2 \pm 0.7^*$	$8.2 \pm 1.0^{\dagger}$
Doppler	0.7 ± 0.2	$4.9 \pm 0.6^*$	$7.8 \pm 0.7^{\dagger}$
Postsystolic shortening, Cx region, %			
Sonomicrometry \ddagger	0.9 ± 0.4	0.9 ± 0.4	0.5 ± 0.3
Doppler \ddagger	1.0 ± 0.2	0.9 ± 0.3	1.4 ± 0.7
Pressure–segment length, loop area, relative value, %			
LAD region	100 ± 0	$33 \pm 6^*$	$-44 \pm 16^{\dagger}$
Cx region \ddagger	100 ± 0	93 ± 7	94 ± 13

Values are mean \pm SEM. Cx indicates circumflex.

* $P < 0.05$ vs baseline; $\dagger P < 0.05$ vs LAD stenosis; $\ddagger n = 9$.

During LAD occlusion, the LV pressure–segment length loop rotated clockwise, resulting in a net negative loop area. However, after short-term ischemia (< 3 minutes), the IVR portion of the pressure–segment length relationship was shifted upwards (by 14.0 ± 2.4 mm Hg). After > 5 minutes of occlusion, the upward shift was abolished, and after 30 minutes with coronary occlusion, there was even a slight downward shift of the IVR portion of the loop (-2.5 ± 2.9 mm Hg).

In each of the experiments in which we calculated regional wall stress, the LV stress–segment length loops confirmed the results from the pressure–dimension analysis. Results were essentially similar for the longitudinal and average stress estimates (Figure 5).

Validation of SDE

Figure 6 displays individual data and demonstrates that peak systolic and peak postsystolic shortening by Doppler correlates well with sonomicrometry ($r=0.90$, $P < 0.01$ and $r=0.83$, $P < 0.01$). Agreement between the two methods is presented as Bland-Altman plots in the same figure.

Reproducibility of SDE

Randomly selected images from all types of interventions were analyzed by 2 observers, and the mean difference

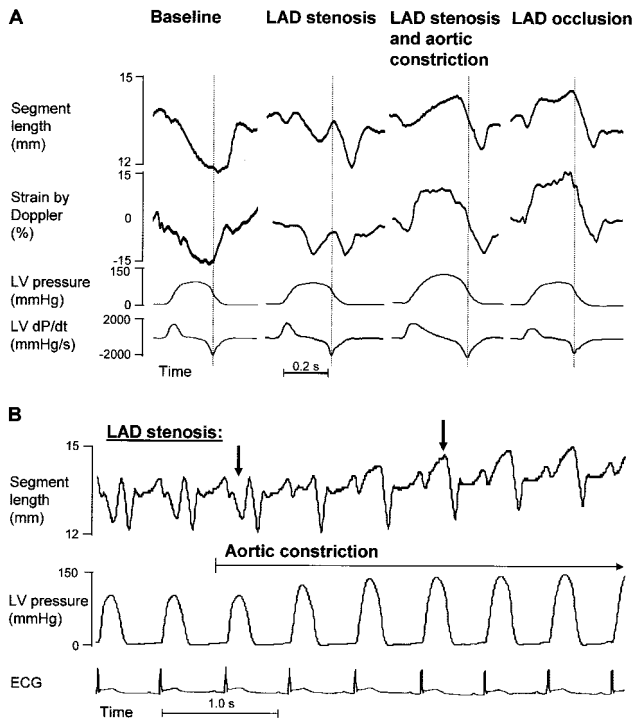


Figure 3. Ischemia and loading-induced changes in regional myocardial contraction patterns in a representative experiment. A, LAD stenosis caused hypokinesia with postsystolic shortening, whereas LAD occlusion caused dyskinesia with even more marked postsystolic shortening. When LAD stenosis was combined with aortic constriction, the contractile pattern resembled that during LAD occlusion. B, Temporal relationship between afterload and contractile pattern. Aortic constriction was superimposed on LAD stenosis, and after 2 beats, systolic shortening turned to systolic lengthening (arrows).

(\pm SD) between observers in peak systolic and postsystolic strain was $0.2 \pm 3.1\%$ and $-0.1 \pm 1.2\%$, indicating no significant systematic difference. The interobserver variability was $-0.3 \pm 2.3\%$ (mean \pm SD) and $-0.1 \pm 1.3\%$, respectively, and beat-to-beat variability in peak systolic and postsystolic strain was $0.6 \pm 2.5\%$ and $1.9 \pm 1.9\%$.

Discussion

Postsystolic shortening has been observed in patients with acute myocardial infarction^{3,4} and during ischemia induced by coronary balloon angioplasty.⁹ In the present study, we reproduced these observations in a dog model of acute myocardial ischemia. Furthermore, we extend the findings of Urheim et al⁸ by showing that SDE has the ability to measure myocardial contractile pattern and to quantify postsystolic shortening.

Our experiments demonstrate that postsystolic contraction occurs during both moderate ischemia, when the myocardium is hypokinetic or akinetic, and during severe ischemia, when the myocardium is dyskinetic. This is consistent with previous studies in different animal models.^{15–18} As demonstrated in the present study, the relationship between regional myocardial deformation and severity of ischemia is not that clear. Whether an ischemic myocardial segment is hypokinetic or dyskinetic depends on the balance between the stress imposed on that segment and the sum of the active and passive stresses

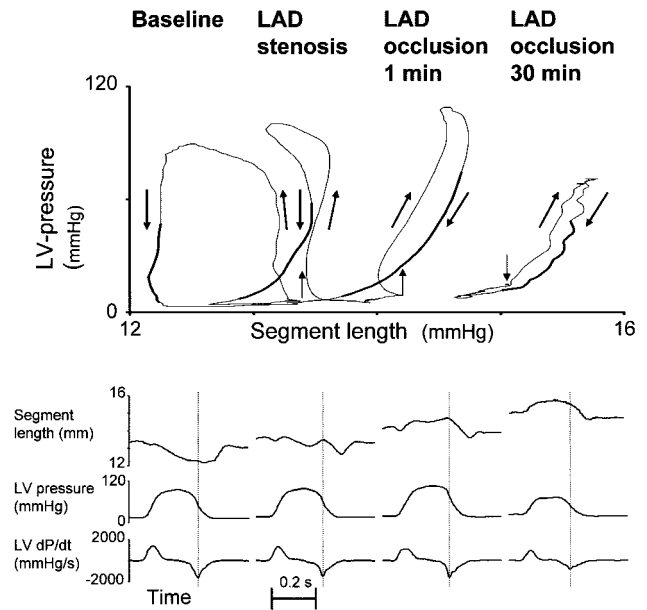


Figure 4. Ischemia-induced changes in LV pressure–segment length relations in a representative experiment. The upper panel displays LV pressure–segment length loops from the recordings in the lower panel. The portions of the loops that are displayed with thick lines represent the IVR period. During LAD stenosis and after 1 minute of LAD occlusion, the pressure–segment length relationship during IVR is shifted upwards (minor arrows) relative to the late diastolic portions of the loops. After 30 minutes with LAD occlusion, however, there is a slight rightward and downward shift during IVR. During baseline and during LAD stenosis, the loops rotate counter-clockwise (arrows), whereas during LAD occlusion, the loops rotate clockwise.

within the segment. This principle was illustrated by the responses to an acute elevation of afterload, which caused an immediate change from hypokinesia to dyskinesia. Because this change occurred instantly, it could not be attributed to aggravation of ischemia or reflex mechanisms but most likely was a pure mechanical effect of elevated afterload. Thus, when the imposed load exceeds the combined active and passive stresses, the ischemic segment behaves as a net passive structure. Therefore, the contractile patterns of ischemic myocardium are strongly influenced by loading conditions, and myocardium that generates active stress may become dyskinetic when afterload exceeds a critical level. For that reason, the finding of dyskinesia may not allow to rule out actively contracting myocardium.

Mechanism of Postsystolic Shortening in Dyskinetic Myocardium

Because a dyskinetic myocardial segment lengthens when LV pressure is rising and shortens when LV pressure is falling, it is dominantly passive. This is analogous to a spring that is stretched; it will shorten passively when the stretching force is removed. The finding of a negative area of the pressure–segment length loop confirms that the segment is net passive, and the loop area reflects work that is performed on that segment by other myocardial segments. The fact that a passive pressure–segment length loop rotates clockwise instead of moving up and down a straight line is attributable to viscoelastic properties of myocardial tissue, and the area of

TABLE 2. Hemodynamic and Strain Variables During Baseline, LAD Stenosis, LAD Stenosis With Aortic Constriction, and LAD Occlusion (n=7)

	Baseline	LAD Stenosis	LAD Stenosis and Aortic Constriction	LAD Occlusion
Heart rate, min ⁻¹	104±9	101±9	90±9*†	99±9
LV peak systolic pressure, mm Hg	102±12	101±10	165±11*†‡	108±11
LV end-diastolic pressure, mm Hg	10±2	10±2	14±2*†	12±2*†
LV dP/dt _{max} , mm Hg/s	1632±172	1400±124	1896±118	1545±205
LAD flow, mL/min	14±2	8±2*	21±6*‡	0±0*†
End-diastolic segment length, mm	10.0±1.6	10.0±1.6	10.2±1.7	10.4±1.7*†
Systolic shortening, %				
Sonomicrometry	11.6±1.2	6.6±1.1*	-8.3±2.3*†	-5.5±0.6*†
Doppler	12.3±1.1	6.6±1.3*	-7.0±0.8*†	-7.9±1.2*†
Postsystolic shortening, %				
Sonomicrometry	1.1±0.4	4.5±0.9*	9.9±2.5*†	8.7±1.4*†
Doppler	0.9±0.2	5.1±0.9*	9.6±1.6*†	8.2±0.4*†
Pressure-segment length, loop area, relative value, %	100±0	37±7*†	-23±17*†‡	-38±13*†

Values are mean±SEM.

**P*<0.05 vs baseline; †*P*<0.05 vs LAD stenosis; ‡*P*<0.05 vs LAD occlusion.

the loop reflects the mechanical energy that is lost because of viscous friction. However, this reasoning does not exclude that a smaller component of active contraction contributes to postsystolic shortening in a dominantly passive segment. The most direct evidence of an active component would be the demonstration of increased myocardial stiffness during postsystolic shortening compared with the stiffness of the fully relaxed myocardium. In the present study, we used regional pressure-segment length relationships and stress-segment length relationships to assess regional myocardial stiffness.

After 1 to 2 minutes of LAD occlusion, the ischemic segment demonstrated net passive motion. However, the pressure-segment length loop indicated a significant contribution from active contraction to postsystolic shortening. The active component was evident as an upward shift of the pressure-segment length loop during postsystolic shortening compared with the late diastolic portion of the same loop. This upward shift implies that a larger pressure is needed to distend the segment during postsystolic shortening than predicted by the passive pressure-segment length relation. This in turn implies that there must be a component of active stress superimposed on the passive stress that results from stretching of the segment in the preceding systole.

One important objection to this reasoning is that abnormal wall thickness, geometry, or effects attributable to tethering to neighboring segments could make pressure an imperfect substitute for stress. To respond to this potential objection, we calculated regional wall stress from simultaneous measurements of pressure, wall thickness, and local myocardial radii of curvature. It was not entirely clear which model best approximates regional wall stress, and we therefore calculated stress using two different approaches. In this model of hyperacute severe ischemia, the stress-segment length analysis using both stress estimates confirmed the pressure-segment length data. Therefore, in dyskinetic myocardium resulting from short-term ischemia, postsystolic shortening

was attributable to a combination of active fiber shortening and passive recoil. However, after >3 to 5 minutes of severe ischemia, the pressure-segment length relationship during postsystolic shortening was shifted rightwards and downwards relative to the late-diastolic segment of the same loop. This implies that less pressure was required to distend the myocardium during postsystolic shortening than in late diastole and is consistent with viscoelastic behavior of an entirely passive segment. Similar findings were done with the stress-segment length analysis. These findings exclude any significant active component to wall stress during postsystolic shortening with LAD occlusion for >3 to 5 minutes.

Mechanism of Postsystolic Shortening in Myocardium With Systolic Hypokinesia or Akinesia

Hypokinetic myocardium demonstrated a characteristic biphasic pattern with shortening during early and mid-systole, lengthening in late systole, and then postsystolic shortening. Because the myocardium was shortening during systole, while LV pressure was rising, there was obviously active contraction. The postsystolic shortening, however, occurred while LV pressure was falling, and therefore additional analysis was required to differentiate between passive recoil and active contraction. During postsystolic shortening, the regional LV pressure-segment length and stress-segment length relationships were shifted markedly upwards relatively to the fully relaxed segment, strongly supporting a substantial contribution from active contraction. The late systolic myocardial lengthening indicates that the postsystolic shortening was in part attributable to passive recoil. A similar pattern with late systolic lengthening has been observed in papillary muscle preparations exposed to hypoxemia.¹⁹

Similarly, in myocardium with systolic akinesia, the pressure-segment length loop analysis indicated an active stress component that contributed to postsystolic shortening. The following qualitative approach is consistent with these inter-

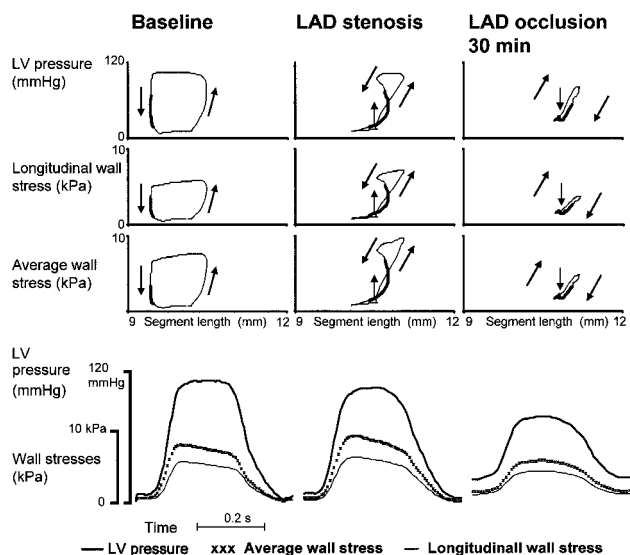


Figure 5. Ischemia-induced changes in LV regional wall stress-segment length relations in a representative experiment. The portions of the loops that are displayed with thick lines represent the IVR period. Similar to the pressure-segment length relationships, the stress-segment length relationships during IVR during LAD stenosis are shifted upward (minor arrows) relative to the late diastolic portions of the loops. After 30 minutes with LAD occlusion, there is a slight rightward and downward shift of the pressure-segment length as well as the stress-segment length relationships during IVR. The arrows indicate the direction of loop rotation. In the lower panel, the separate traces of LV pressure and wall stresses are displayed.

pretations: A segment that does not deform during the substantial rise in LV pressure during isovolumic contraction, but shortens markedly when pressure is falling during isovolumic relaxation, is not likely to be passive. A passive

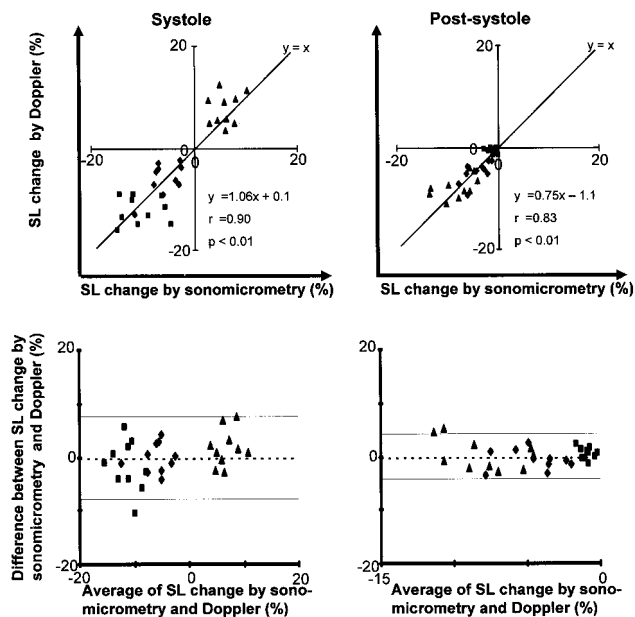


Figure 6. Comparisons between systolic and postsystolic shortening by SDE versus sonomicrometry. Correlations are displayed in upper panels and agreement plots in lower panels. Mean difference \pm 2 SD is indicated. ■ indicates baseline; ◆, LAD stenosis; ▲, LAD occlusion.

myocardial segment should distend as much when pressure is rising during isovolumic contraction as when pressure is falling by a similar magnitude during isovolumic relaxation. Therefore, a segment that demonstrates both systolic akinesia and postsystolic shortening is likely to be actively contracting and therefore viable.

Limitations

The present animal model was heavily instrumented, and this may have influenced measurements and responses to interventions. However, we were able to reproduce the clinical observation of postsystolic shortening in ischemic myocardium. Therefore, we believe the present model is valid for studying mechanisms of postsystolic shortening during acute myocardial ischemia.

The present study was limited to acute changes in myocardial function, and the duration of ischemia was no more than 30 minutes. This limitation implies that we studied myocardium that was predominantly viable. In a clinical setting it is essential to know how contractile patterns develop over much longer periods of time and to determine the relationship between contractile patterns and recovery of function after reperfusion.

Individual variability in coronary artery collateral flow is a general problem with dog models of ischemia. In the present study, however, we reduced this problem by standardizing the mechanical response to ischemia by reducing coronary artery flow as much as we needed to get marked hypokinesia.

An important limitation of SDE is marked angle dependency, which makes it very sensitive to malalignment between the principle direction of myocardial shortening and the Doppler beam. This problem was easily taken care of in the present open chest animal preparation but may be more complicated in a clinical intensive care setting. Furthermore, when applied clinically, the strain images may be quite noisy because of suboptimal image quality. This problem could hopefully be reduced by improvements in filtering and signal-averaging algorithms.

Conclusion

The present study demonstrates that postsystolic shortening is an important feature of ischemic myocardium, and when associated with systolic hypokinesia or akinesia, it indicates actively contracting and, therefore, potentially viable myocardium. When combined with dyskinesia, however, postsystolic shortening seems to be a nonspecific marker of severe ischemia. Strain Doppler echocardiography has the ability to quantify contractile function in ischemic myocardium, and clinical studies should be done to determine if this approach might be useful in patients with acute myocardial infarction.

Acknowledgments

Drs Skulstad, Edvardsen, Urheim, and Lyseggen are recipients of a clinical research fellowship from the Norwegian Council on Cardiovascular Diseases. Dr Rabben is a recipient of a postdoctoral research fellowship from the Research Council of Norway. We thank engineer Roger Ødegaard for important technical assistance.

References

1. Brown MA, Norris RM, Takayama M, et al. Postsystolic shortening: a marker of potential for early recovery of acutely ischaemic myocardium in the dog. *Cardiovasc Res*. 1987;21:703–716.
2. Takayama M, Norris RM, Brown MA, et al. Postsystolic shortening of acutely ischemic canine myocardium predicts early and late recovery of function after coronary artery perfusion. *Circulation*. 1988;78:994–1007.
3. Gibson D, Mehmel H, Schwarz F, et al. Changes in left ventricular regional asynchrony after intracoronary thrombolysis in patients with impending myocardial infarction. *Br Heart J*. 1986;56:121–130.
4. Hosokawa H, Sheehan FH, Suzuki T. Measurement of postsystolic shortening to assess viability and predict recovery of left ventricular function after acute myocardial infarction. *J Am Coll Cardiol*. 2000;35:1842–1849.
5. Mirsky I, Pasternac A, Ellison RC. General index for the assessment of cardiac function. *Am J Cardiol*. 1972;30:483–491.
6. Quinones MA, Gaasch WH, Alexander JK. Echocardiographic assessment of the left ventricular function with special reference to normalized velocities. *Circulation*. 1974;50:42–51.
7. Heimdahl A, Støylen A, Torp H, et al. Real-time strain rate imaging of the left ventricle by ultrasound. *J Am Soc Echocardiogr*. 1998;11:1013–1019.
8. Urheim S, Edvardsen T, Torp H, et al. Myocardial strain by Doppler echocardiography: validation of a new method to quantify regional myocardial function. *Circulation*. 2000;102:1158–1164.
9. Jamal F, Kukulski T, D'Hooge J, et al. Abnormal postsystolic thickening in acutely ischemic myocardium during coronary angioplasty: a velocity, strain, and strain rate Doppler myocardial imaging study. *J Am Soc Echocardiogr*. 1999;12:994–946.
10. Edvardsen T, Urheim S, Skulstad H, et al. Quantification of left ventricular systolic function by tissue Doppler echocardiography: added value of measuring pre- and post-ejection velocities in ischemic myocardium. *Circulation*. 2002;105:2071–2077.
11. Regen DM. Calculation of left ventricular wall stress. *Circ Res*. 1990;67:245–252.
12. DeAnda A, Komeda M, Moon MR, et al. Estimation of regional left ventricular wall stresses in intact canine hearts. *Am J Physiol*. 1998;275:H1879–H1885.
13. Rabben SI, Irgens F, Angelsen B. Equations for estimating muscle fiber stress in the left ventricular wall. *Heart Vessels*. 1999;14:189–196.
14. Bland JM, Altman DG. Statistical methods for assessing agreement between two methods of clinical measurement. *Lancet*. 1986;8:307–310.
15. Waters DD, Da Luz P, Wyatt HL, et al. Early changes in regional and global left ventricular function induced by graded reductions in regional coronary perfusion. *J Am Coll Cardiol*. 1977;39:537–543.
16. Safwat A, Leone BJ, Norris RM, et al. Pressure-length loop area: its components analyzed during graded myocardial ischemia. *J Am Coll Cardiol*. 1991;17:790–796.
17. Derumeaux G, Ovize M, Loufoua J, et al. Doppler tissue imaging quantitates regional wall motion during myocardial ischemia and reperfusion. *Circulation*. 1998;97:1970–1977.
18. Jamal F, Strotmann J, Weidemann F, et al. Noninvasive quantification of the contractile reserve of stunned myocardium by ultrasonic strain rate and strain. *Circulation*. 2001;104:1059–1065.
19. Wiegner AW, Allen GJ, Bing OHL. Weak and strong myocardium in series: implications for segmental dysfunction. *Am J Physiol*. 1978;235:H776–H783.